



HAL
open science

Palaeogeography of a shallow carbonate platform: The case of the Middle to Late Oxfordian in the Swiss Jura Mountains

Andre Strasser, Bernard Pittet, Wolfgang Hug

► **To cite this version:**

Andre Strasser, Bernard Pittet, Wolfgang Hug. Palaeogeography of a shallow carbonate platform: The case of the Middle to Late Oxfordian in the Swiss Jura Mountains. *Journal of Palaeogeography-English*, 2015, 4 (3), pp.251-268. 10.1016/j.jop.2015.08.005 . hal-02341072

HAL Id: hal-02341072

<https://univ-lyon1.hal.science/hal-02341072>

Submitted on 15 Sep 2021

HAL is a multi-disciplinary open access archive for the deposit and dissemination of scientific research documents, whether they are published or not. The documents may come from teaching and research institutions in France or abroad, or from public or private research centers.

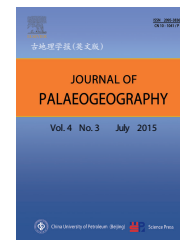
L'archive ouverte pluridisciplinaire **HAL**, est destinée au dépôt et à la diffusion de documents scientifiques de niveau recherche, publiés ou non, émanant des établissements d'enseignement et de recherche français ou étrangers, des laboratoires publics ou privés.



Distributed under a Creative Commons Attribution 4.0 International License

Available online at www.sciencedirect.com

ScienceDirect

journal homepage: <http://www.journals.elsevier.com/journal-of-palaeogeography/>

Lithofacies palaeogeography and sedimentology

Palaeogeography of a shallow carbonate platform: The case of the Middle to Late Oxfordian in the Swiss Jura Mountains



André Strasser^{a, *}, Bernard Pittet^b, Wolfgang Hug^c

^a Department of Geosciences, University of Fribourg, Chemin du Musée 6, 1700 Fribourg, Switzerland

^b Université Lyon 1, UMR CNRS LGLTPE 5276, Campus Doua, Bâtiment Géode, 69622 Villeurbanne, France

^c Paléontologie A16, Section d'archéologie et paléontologie, Office de la culture, Hôtel des Halles, 2900 Porrentruy, Switzerland

Received 6 November 2014; accepted 17 April 2015

KEYWORDS

Swiss Jura,
Oxfordian,
carbonate platform,
facies evolution,
sequence stratigraphy,
cyclostratigraphy

Abstract The Oxfordian (Late Jurassic) carbonate-dominated platform outcropping in the Swiss Jura Mountains offers a good biostratigraphic, sequence-stratigraphic, and cyclostratigraphic framework to reconstruct changes in facies distribution at a time-resolution of 100 ka. It thus allows interpreting the dynamic evolution of this platform in much more detail than conventional palaeogeographic maps permit. As an example, a Middle to Late Oxfordian time slice is presented, spanning an interval of about 1.6 Ma. The study is based on 12 sections logged at cm-scale. The interpreted depositional environments include marginal-marine emerged lands, fresh-water lakes, tidal flats, shallow lagoons, ooid shoals, and coral reefs. Although limestones dominate, marly intervals and dolomites occur sporadically.

Major facies shifts are related to m-scale sea-level changes linked to the orbital short eccentricity cycle (100 ka). The 20-ka precession cycle caused minor facies changes but cannot always be resolved. Synsedimentary tectonics induced additional accommodation changes by creating shallow basins where clays accumulated or highs on which shoals or islands formed. Autocyclic processes such as lateral migration of ooid and bioclastic shoals added to the sedimentary record. Climate changes intervened to control terrestrial run-off and, consequently, siliciclastic and nutrient input. Coral reefs reacted to such input by becoming dominated by microbialites and eventually by being smothered. Concomitant occurrence of siliciclastics and

* Corresponding author.

E-mail address: andreas.strasser@unifr.ch.

Peer review under responsibility of China University of Petroleum (Beijing).

dolomite in certain intervals further suggests that, at times, it was relatively arid in the study area but there was rainfall in more northern latitudes, eroding the Hercynian substrate.

These examples from the Swiss Jura demonstrate the highly dynamic and (geologically speaking) rapid evolution of sedimentary systems, in which tectonically controlled basin morphology, orbitally induced climate and sea-level changes, currents, and the ecology of the carbonate-producing organisms interacted to form the observed stratigraphic record. However, the interpretations have to be treated with caution because the km-wide spacing between the studied sections is too large to monitor the small-scale facies mosaics as they can be observed on modern platforms and as they certainly also occurred in the past.

1 Introduction

Palaeogeographic maps based on plate-tectonic reconstructions and covering large areas (*e.g.*, Blakey, 2014; Scotese, 2014; Stampfli and Borel, 2002; Stampfli *et al.*, 2013) are very useful to visualize the general context in which a study area evolved. However, coastlines and facies distributions then are often presented time-averaged over million-year long time intervals (*e.g.*, Dercourt *et al.*, 1993). In the case of shallow carbonate platforms where facies patterns change rapidly through time as well as through space (facies mosaics; *e.g.*, Rankey and Reeder, 2010; Wilkinson and Drummond, 2004), it is useful to search for a more detailed picture of palaeogeography.

The goal of this study is to present a series of maps that monitor the facies evolution of an ancient carbonate platform in (geologically speaking) narrow time-steps. As an example, a time interval in the Oxfordian (Late Jurassic) of the Swiss Jura Mountains is chosen. The controlling mechanisms of facies distribution in time and in space will be discussed, and the potential and limitations of such an approach to palaeogeography will be evaluated.

2 Palaeogeographic and stratigraphic setting

In Middle to Late Oxfordian times, a wide, carbonate-dominated shelf covered the realm of today's Jura Mountains (Fig. 1). It was structured by differential subsidence along faults inherited from older lineaments (Wetzel *et al.*, 1993; Wetzel and Allia, 2000). To the north, very shallow depositional environments predominated, whereas to the south deeper epicontinental basins developed. Siliciclastic material was furnished episodically by the erosion of Hercynian crystalline massifs in the hinterland. The study area was situated at a palaeolatitude estimated between 33°N and 38°N (Barron *et al.*, 1981; Dercourt *et al.*, 1993; Smith *et al.*, 1994).

Lithostratigraphy and facies of the Oxfordian in the Swiss Jura Mountains have been studied extensively by, *e.g.*, Ziegler (1956, 1962), Gygi (1969, 1992), and Bolliger and Burri (1970). The biostratigraphy based on ammonites was established mainly by Gygi (1995, including summary of earlier work). Gygi and Persoz (1986) used bio- and mineral stratigraphy to reconstruct the platform-to-basin transition. A correlation with the French Jura was established by Enay *et al.* (1988); a sequence-stratigraphic interpretation has been proposed by Gygi *et al.* (1998). Selected intervals calibrated by high-resolution sequence stratigraphy and

cyclostratigraphy have been analyzed and interpreted by Pittet (1996), Dupraz (1999), Hug (2003), Védérine (2007), and Stienne (2010). Jank *et al.* (2006) presented a comprehensive view of Late Oxfordian to Kimmeridgian stratigraphy and palaeogeography. The formation of platform and basin facies in space and time and their relationship to synsedimentary tectonics was analyzed in detail by Alenbach (2001).

The terminology of formations and members and their biostratigraphic attribution follow Gygi (1995, 2000; Fig. 2). The major sequence boundaries are labeled according to Hardenbol *et al.* (1998), and the numerical ages are based on Gradstein *et al.* (1995). Although a more recent geological time-scale is available (International Commission on Stratigraphy, 2014), we use the older one because the ages of ammonite zones and sequence boundaries in the chart of Hardenbol *et al.* (1998) are interpolated using the numbers of Gradstein *et al.* (1995).

3 Methods

The sections presented here (Fig. 3 and Table 1) have been logged at cm-scale. Dense sampling guaranteed that even minor facies changes were detected. Thin-sections were prepared for the rock samples; marls were washed and the residue picked for microfossils. Under the optical microscope or the binocular, microfacies have been analyzed using the Dunham (1962) classification for carbonate rocks and a semi-quantitative estimation of the abundance of rock constituents (Fig. 4). Special attention has been paid to sedimentary structures and to omission surfaces (*cf.* Clari *et al.*, 1995; Hillgärtner, 1998). The sum of this sedimentological information was then used to interpret the depositional environments. For the sequence-stratigraphic interpretation of the facies evolution, the nomenclature of Vail *et al.* (1991) was applied. Vertical facies changes define deepening-shallowing depositional sequences, which are hierarchically stacked (example in Fig. 4).

Elementary sequences are the smallest units where facies evolution indicates a cycle of environmental change, including sea-level change (Strasser *et al.*, 1999). In some cases, there is no facies evolution discernable within a bed but marls or omission surfaces delimiting the bed suggest an environmental change (Strasser and Hillgärtner, 1998). Commonly, 2 to 7 elementary sequences compose a small-scale sequence, which generally displays a deepening then shallowing trend and exhibits the relatively shallowest facies at its boundaries (Fig. 4). For example, birdseyes, mi-

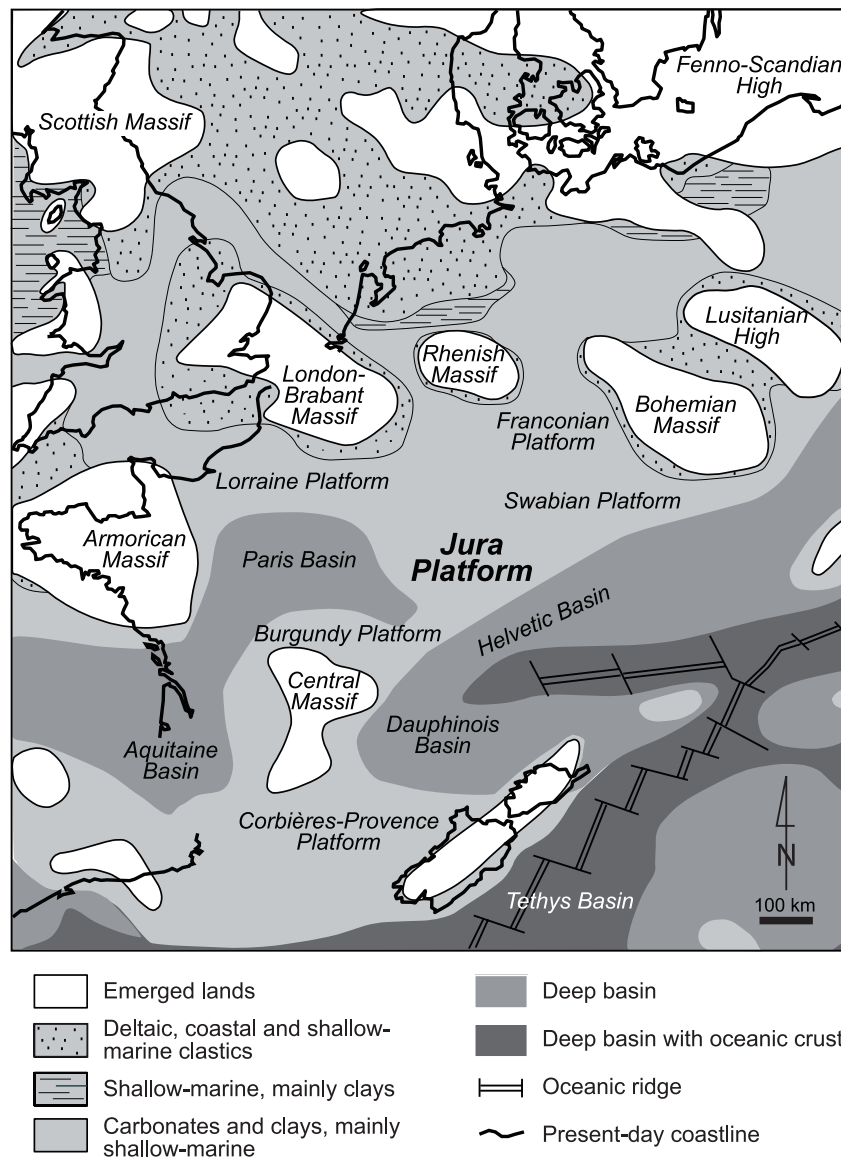


Figure 1 Palaeogeographic setting of the Jura Platform during the Oxfordian. Modified from Carpentier *et al.* (2006), based on Enay *et al.* (1980), Ziegler (1988), and Thierry (2000).

crobbial mats, or penecontemporaneous dolomitization suggest tidal-flat environments, keystone vugs in grainstones point to a beach, and detrital quartz grains and plant fragments indicate input from the hinterland during low relative sea level (late highstand and/or early transgressive conditions; Pittet and Strasser, 1998). In the studied sections it is common that four small-scale sequences make up a medium-scale sequence, which again displays a general deepening-shallowing trend of facies evolution and the relatively shallowest facies at its boundaries. Furthermore, the elementary sequences commonly are thinner around the small-scale and medium-scale sequence boundaries, which suggests reduced accommodation. Thick elementary sequences in the central parts of these sequences imply higher accommodation.

Based on these interpretations, and within the biostratigraphic and sequence-stratigraphic framework (Fig. 2), the studied sections have been correlated at the scale of the

small-scale sequences (Fig. 5; Strasser, 2007). Although this correlation includes uncertainties as to where exactly place some small-scale sequence boundaries, it nevertheless offers the basis for a general palaeogeographic interpretation with a relatively high time resolution. The dominant facies category has been interpreted for each deepening-upward (transgressive) and each shallowing-upward (regressive) part of each small-scale sequence (dominant meaning that over 50% of the non-decompacted facies thickness encountered in one part can be attributed to that category).

4 Facies and depositional environments

The detailed analysis of the microfacies encountered in the studied sections and the interpretation of the depositional environments has been performed by Pittet (1996), Dupraz (1999), Gsponer (1999), Jordan (1999), Rauber (2001),

Chronostrat.	Biostratigraphy		Sequence boundaries	Lithostratigraphy (Swiss Jura)	
	ammonite zones	subzones			
Tithonian	Hybonotum		Ti 1	Twannbach Fm.	
		Kimmeridgian	Autissiodorensis	Kim 5	Upper Virgula Mb.
Eudoxus	Kim 4		Lower Virgula Mb.		
Acanthicum	Kim 3		Banné Mb.		
Divisum	Kim 2		Reuchenette Fm.		
Hypselocyclum	Kim 1				
Platynota					
Oxfordian	Planula	Galar Planula	Ox 8	Courgenay Fm.	Porrentruy Mb. Verena Mb. Holzfluh Mb.
		Hauffianum	Ox 7	Bure Mb. Oolithe rousse	La May Mb. Laufen Mb.
	Bimammatum	Bimammatum	Ox 6	Hauptmumienbank Mb.	Steinebach Mb.
		Hypselum		Vellerat Fm.	Röschenz Mb. Balsthal Fm. Effingen Mb.
	Bifurcatus	Grossouvrei		Vorbourg Mb.	Günsberg Mb. Wildegge Fm.
		Stenocycloides			
		Rotoides / Schilli	Ox 5	St. Ursanne Fm.	Pichoux Fm. Birmenstorf Mb.
	Transversarium	Luciaef. / Parandieri	Ox 4	Liesberg Mb.	Birmenstorf Mb. (condensed)
			Ox 3	Bärschwil Fm.	(hiatus)
	Plicatilis	Antecedens			
Densiplicatum / Vertebr.					

Figure 2 Chronostratigraphy, biostratigraphy, and lithostratigraphy of the study area. Litho- and biostratigraphic scheme after Gygi (1995, 2000), with circles indicating where biostratigraphically significant ammonites have been found. Sequence boundaries after Hardenbol *et al.* (1998) and Gygi *et al.* (1998). Studied interval in grey. Fm.: Formation; Mb.: Member.

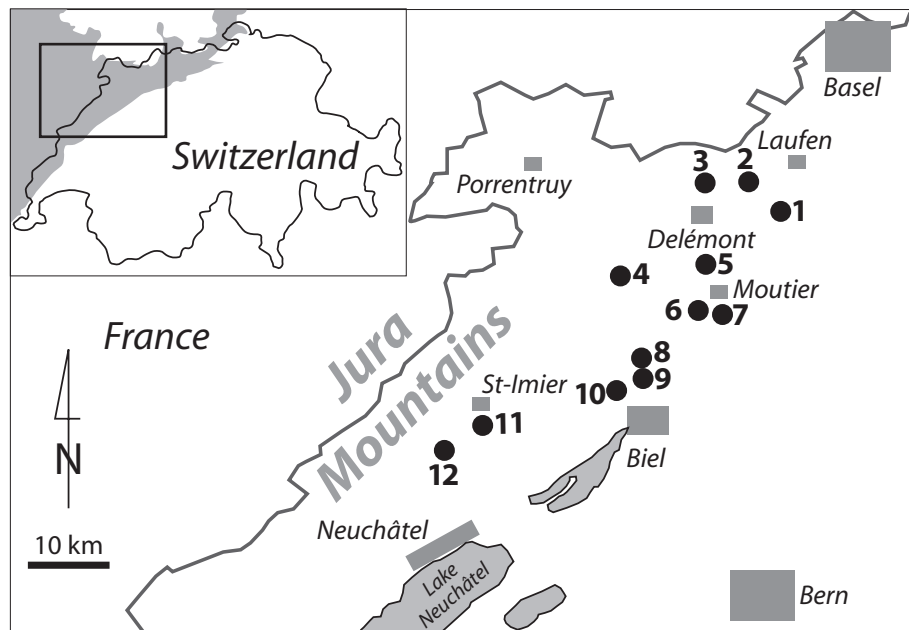


Figure 3 Locations of the studied sections in the Swiss Jura. Inset: Jura Mountains in grey.

and Hug (2003). Lateral facies changes over short distances and vertical changes over short time intervals are common. For example, Samankassou *et al.* (2003) illustrated a close juxtaposition of coral reefs and ooid shoals in the Steinebach Member, and Védrine and Strasser (2009) looked into the distribution of corals, ooids, and oncoids in the Hauptmumienbank and Steinebach members with a time resolution of 20 ka. For the purpose of the present paper, however, only

a very general view of facies is presented, which filters out the local facies changes and permits to illustrate the general palaeogeographical evolution of the study area.

The Dunham (1962) classification, typical grains and fossils, and sedimentary structures are used to interpret the depositional environment in terms of water depth, water energy, and ecological conditions (e.g., oxygenation, nutrients, substrate). The so defined environments are grouped

No. of Section	Name	Location	Stratigraphic interval	Author(s)
1	Les Champés	Along forest road SE of Bärschwil	Middle Oxfordian to Early Kimmeridgian	Rauber (2001)
2	Liesberg	In quarry of cement factory	Late Oxfordian	Hug (2003)
3	Mettemberg-Soyhières	Along road from Mettemberg to Soyhières	Late Oxfordian	Hug (2003)
4	Gorges du Pichoux	Along road between Undervelier and Sornetan	Middle Oxfordian to Late Kimmeridgian	Pittet (1996), Colombié (2002)
5	Hautes Roches	Along forest path south of the village of Hautes Roches	Middle to Late Oxfordian	Pittet (1996), Dupraz (1999)
6	Gorges de Court	Along road and footpath between Moutier and Court	Middle to Late Oxfordian	Pittet (1996), Colombié (2002), Hug (2003)
7	Moutier	Borehole SE of Moutier	Middle to Late Oxfordian	Pittet (1996), Dupraz (1999)
8	La Chamalle	Along forest road to La Chamalle farm	Late Oxfordian	Jordan (1999)
9	Péry-Reuchenette	In quarry of cement factory	Middle Oxfordian to Late Kimmeridgian	Pittet (1996), Colombié (2002), Hug (2003)
10	Forêt de Châtel	Along forest road	Late Oxfordian	Gsponer (1999)
11	Savagnières	Along road between St-Imier and Val-de-Ruz	Middle to Late Oxfordian	Pittet (1996)
12	Pertuis	Along road from Dombresson to Pertuis	Middle to Late Oxfordian	Pittet (1996)

into larger categories that characterized the Oxfordian carbonate platform: (1) emerged land, lake, and beach, (2) tidal flat, (3) restricted lagoon (in terms of reduced energy and/or oxygenation), (4) open lagoon, (5) ooid shoal, and (6) coral reef. Furthermore, significant terrigenous input (siliciclastics and/or plant material) and dolomitization are distinguished. A summary of the facies characteristics of these categories is given in Table 2.

5 Depositional sequences and their timing

The fact that most of the small-scale and medium-scale sequence boundaries can be followed over hundreds of kilometers points to an allocyclic (*i.e.* external) control on sequence formation. However, also autocyclic processes (such as lateral migration of sediment bodies or reactivation of high-energy shoals) occurred and are recorded mainly on the level of the elementary sequences (Hill *et al.*, 2012; Strasser, 1991; Strasser and Vêdrine, 2009).

Based on the lithostratigraphic and biostratigraphic frame furnished by Gygi and Persoz (1986) and Gygi (1995), and on the detailed analyses of stacking pattern and facies evolution, a sequence-stratigraphic and cyclostratigraphic interpretation can be proposed for each studied section. However, superposition of higher-frequency sea-level fluctuations on a long-term trend of sea-level change led to repetition of diagnostic surfaces, defining sequence-boundary zones (Montañez and Osleger, 1993; Strasser *et al.*, 1999). Fast rise of sea level either caused distinct maximum-flooding surfaces (which again may be repeated defining a maximum-flooding zone), or is recorded by the relatively deepest or most open-marine facies. Major transgressive surfaces generally correlate well from one section

to another. The correlation of small-scale sequences is relatively straightforward, although the exact emplacement of their sequence boundaries may be difficult to judge when the elementary sequences are not well defined.

Comparing the interpretation of the studied sections with the sequence stratigraphy of Hardenbol *et al.* (1998) established in European basins, and based on the stratigraphic scheme presented in Figure 2, the large-scale sequence boundaries Ox 6, Ox 7, and Ox 8 can easily be identified. The numerical ages attributed by Hardenbol *et al.* (1998) to these sequence boundaries allow estimating the duration of the small- and medium-scale sequences identified in the studied outcrops, assuming that each sequence of a given order had the same duration. Ox 6 is dated at 155.8 Ma, Ox 8 at 154.6 Ma (Hardenbol *et al.*, 1998). Three medium-scale and 12 small-scale sequences are counted between these sequence boundaries (Fig. 5). It thus can be assumed that a small-scale sequence lasted about 100 ka, and a medium-scale sequence about 400 ka. A best-fit correlation for the Middle Oxfordian to Late Kimmeridgian interval has been proposed by Strasser (2007), which confirms this interpretation. Consequently, it can be concluded that the formation of the observed, hierarchically stacked depositional sequences was at least partly controlled by sea-level changes, which themselves were controlled by climatic changes, and these were induced by orbitally-induced insolation changes. Thus, the small-scale sequences correspond to the short eccentricity cycle of 100 ka, and the medium-scale sequences to the long eccentricity cycle of 400 ka.

Where 5 elementary sequences compose a small-scale one, it can be assumed that also the 20-ka precessional cycle is recorded. However, in many cases the facies evolution within an elementary sequence does not allow demonstrating that it was created by a sea-level cycle (and thus

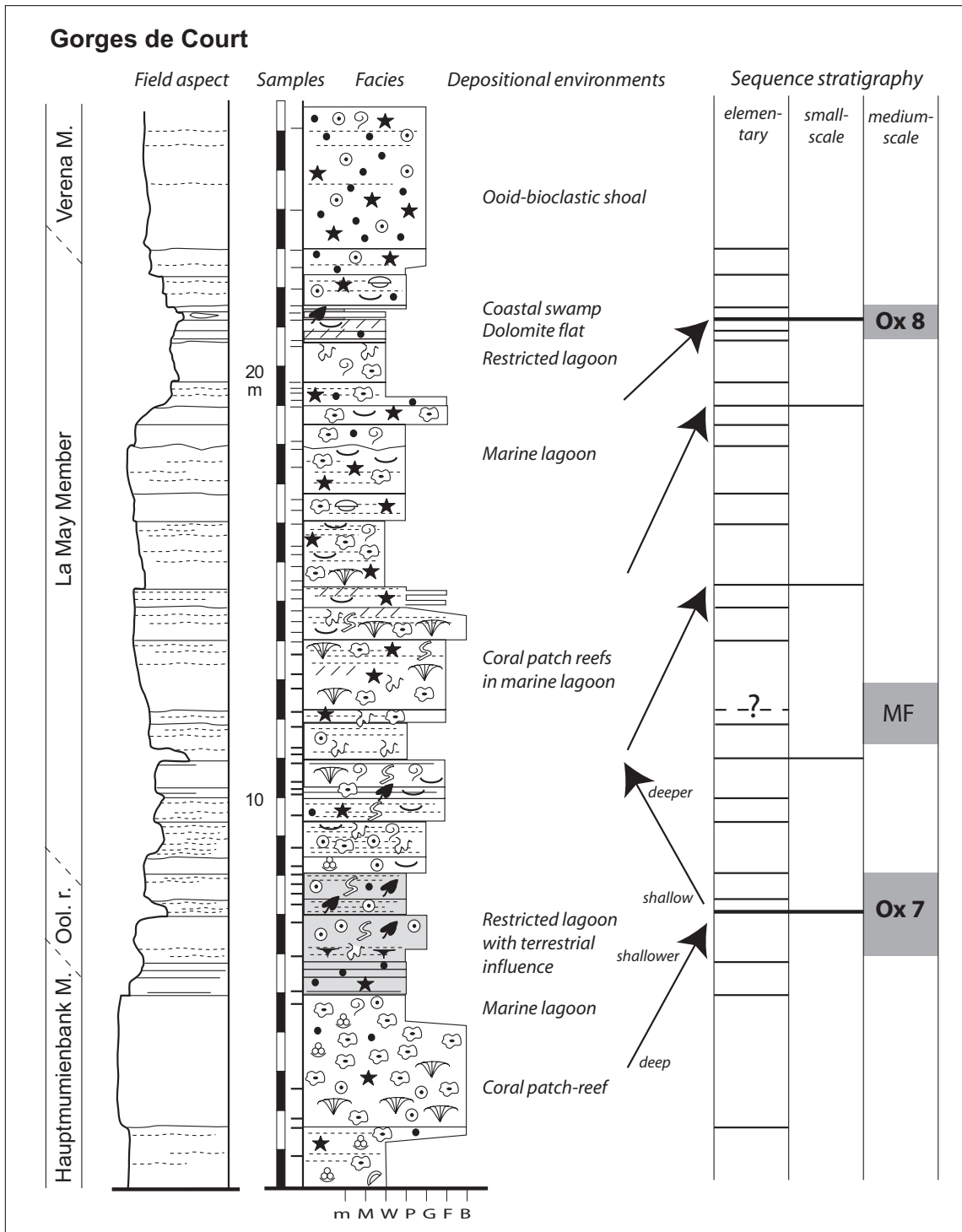


Figure 4 Deepening-shallowing trends of facies evolution, and sequence- and cyclostratigraphic interpretation of a part of the Gorges de Court section (number 6 in Fig. 3). Legend of facies symbols in Figure 5. MF: maximum-flooding interval. Ool. r.: Oolithe rousse Member.

related to an orbital cycle): autocyclic processes may have overprinted the allocyclic signal.

6 Palinspastic reconstruction of the platform

The study area lies in the fold-and-thrust belt of the Jura Mountains, which formed during the Late Miocene to

Early Pliocene. In order to represent the palaeo-distances between the studied sections, a palinspastic reconstruction has been performed. The tectonic structure is complex with broken anticlines and thrust folds, which in the study area generally strike NNE-SSW (Hindle and Burkhard, 1999; Mosar, 1999). Based on the restored cross-sections published by Bitterli (1990), a N-S elongation factor of 1.5 to 2 is assumed when compared to today's geographic posi-

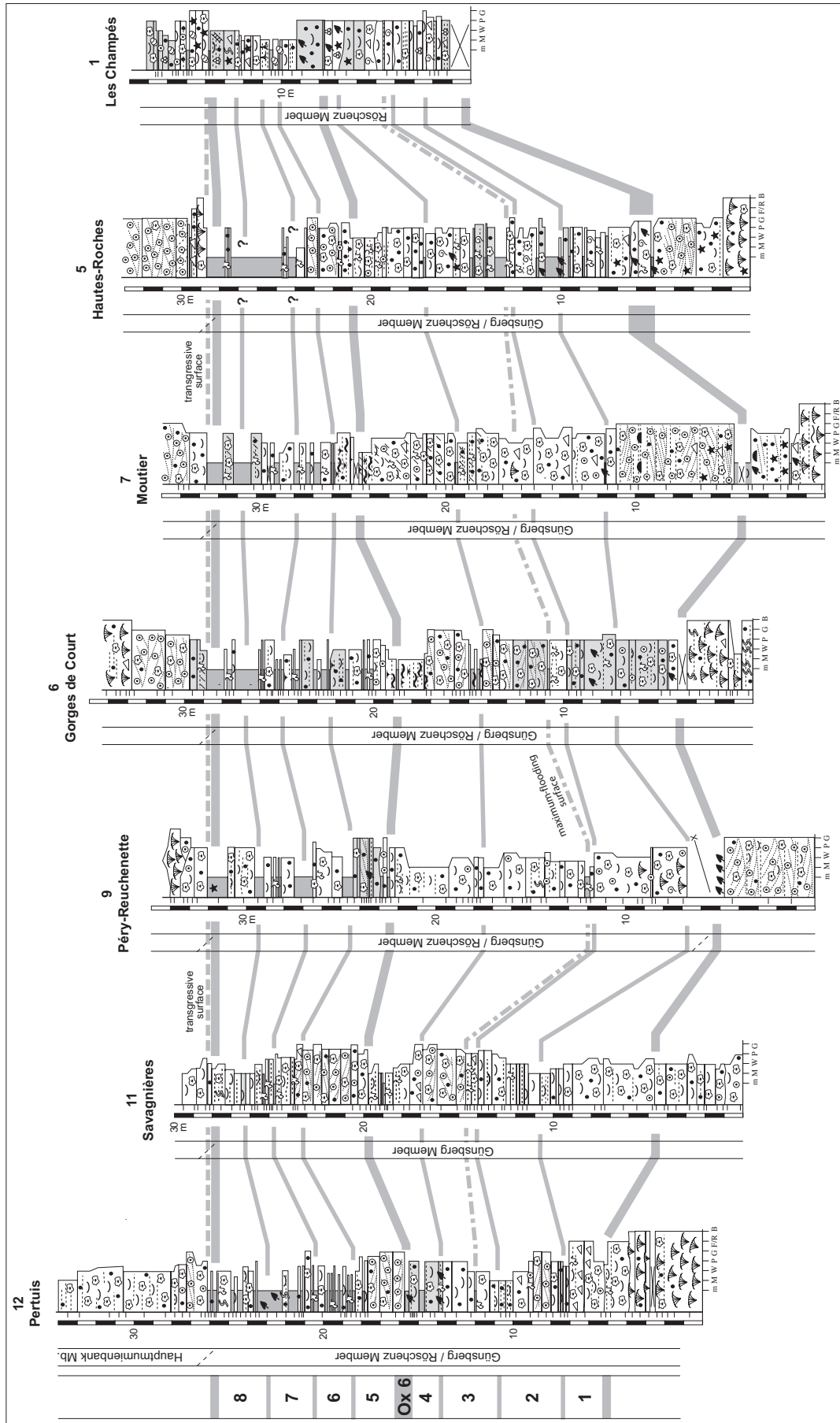


Figure 5 Correlation of small-scale sequences (numbered on the left) between the studied sections.

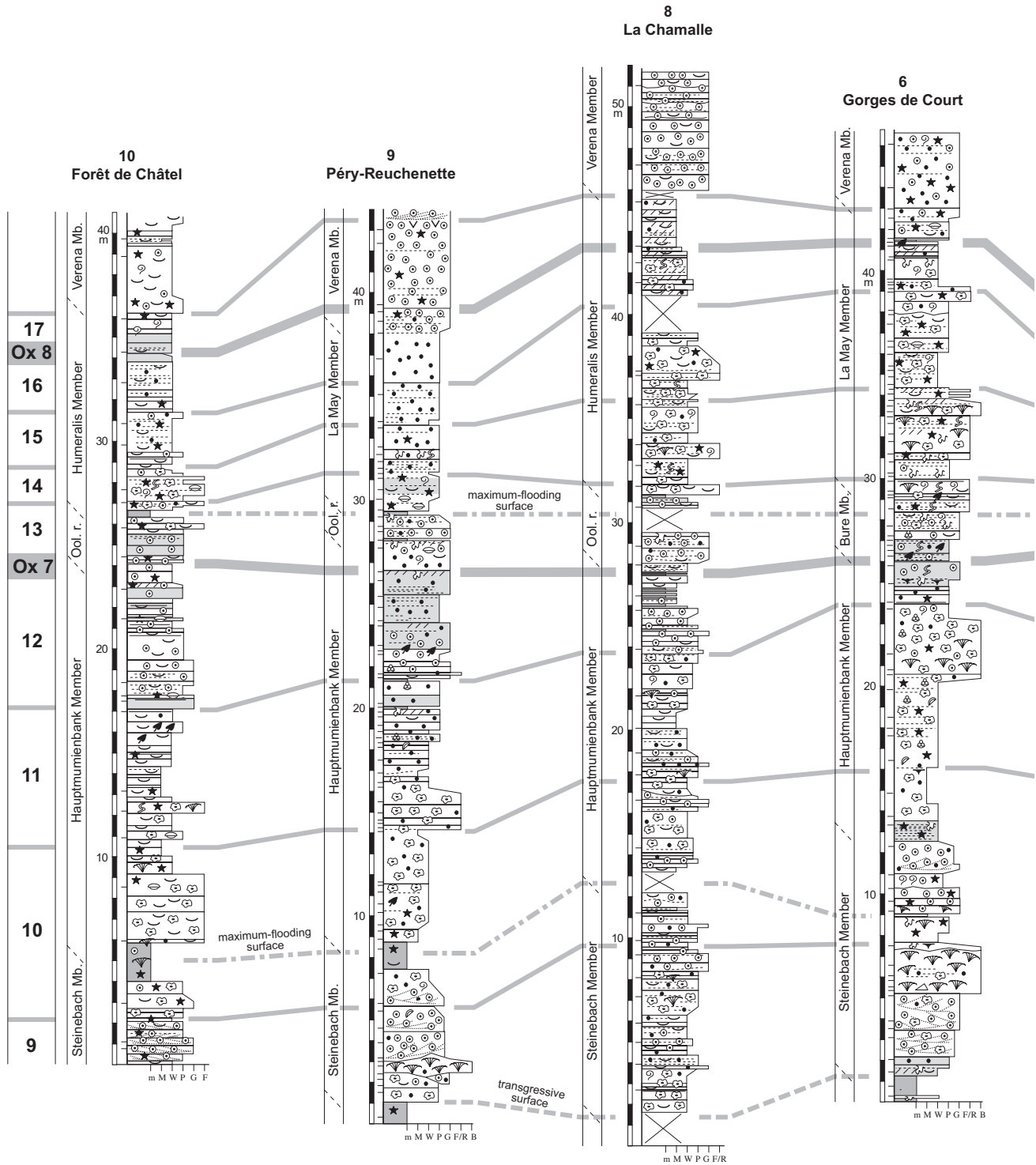


Figure 5, continued.

tion of the sections (Figs 3 and 7). The folds and thrusts are cross-cut by numerous faults, which were mainly inherited from the Paleogene rifting in the Upper Rhine Graben (Ustaszewski and Schmid, 2006). However, the N-S displacement along these faults is negligible in the study area.

The palinspastic map thus established serves as the base for the facies maps presented in chapter 7. Even if there

are many uncertainties about the true palaeo-distances between the sections, their positions relative to each other are preserved.

7 Dynamic evolution of the platform

In order to reconstruct the facies evolution of the

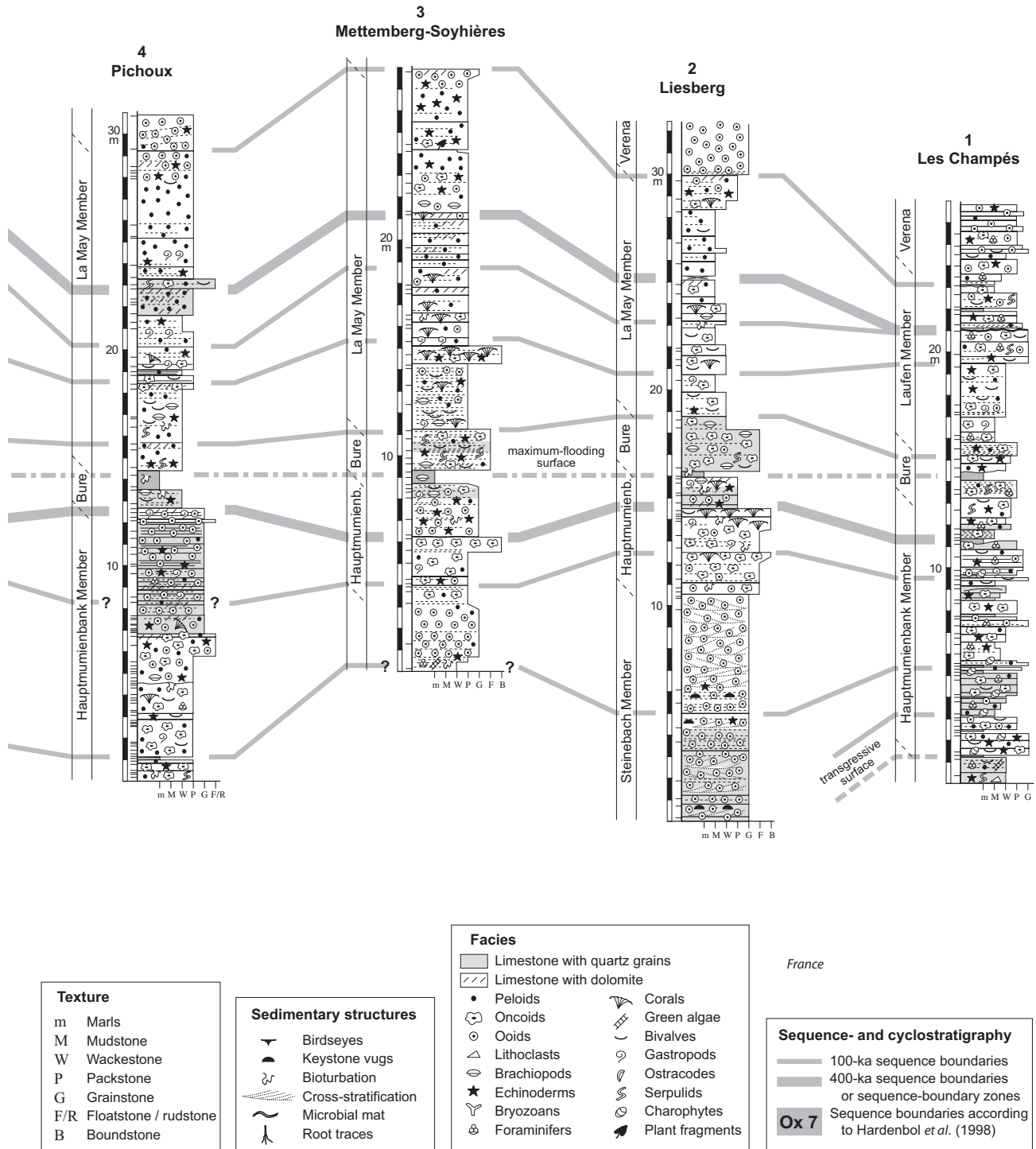


Figure 5, continued.

Jura Platform through space and time, steps of half a small-scale depositional sequence have been chosen. Each sequence numbered in Figure 5 is subdivided into a deepening part (transgressive deposits) and a shallowing, regressive part (highstand deposits; Fig. 6). Lowstand deposits are commonly absent or strongly reduced on the shallow platform. For both parts, the dominant facies category in each section is then reported on the corresponding map. Figure 7 shows 32 such maps. If a small-scale se-

quence is considered to cover 100 ka, an interval of 1.6 Ma is thus represented. It can be assumed that the sea-level fluctuations in the green-house world of the Late Jurassic were more or less symmetrical, in contrast to the strongly asymmetrical sea-level changes related to rapid melting and slow build-up of continental ice in ice-house worlds. Consequently, the transgressive and highstand parts of a small-scale sequence would each correspond to approximately 50 ka, including the hiatuses at the boundaries of

Table 2 Summary of microfacies encountered in the studied sections, interpretation of depositional environments, and definition of facies categories

Dunham classification	Typical particles	Typical fossils	Sedimentary structures	Interpretation	Category
	Lithoclasts	Root traces	Irregular surfaces, hardground	Palaeosol, karst	
M, W, P, marls	Peloids, bioclasts	Charophytes, reworked marine fossils	Bioturbation	Lake	Emerged land, lake, beach
G, P, R	Ooids, peloids, bioclasts (well sorted)	Mixed fauna	Keystone vugs, plane-bed lamination	Beach	
M, W, P, marls	Peloids, mud chips	Gastropods, ostracods	Birdseyes, microbial lamination, desiccation cracks, bioturbation	Tidal flat	Tidal flat
W, P, F, marls	Peloids, bioclasts, soft pebbles,	Benthic forams, echinoderms, bivalves, gastropods, plant fragments	Bioturbation	Tidal channel	
M, W, P, marls	Peloids, oncoids,	Gastropods, miliolids, microencrusters, plant fragments		Closed, strongly restricted lagoon	Restricted lagoon
M, W, P, marls	Peloids, oncoids, ooids, bioclasts	Echinoderms, brachiopods, bivalves, gastropods, green algae, benthic forams, sponges, microencrusters	Flaser bedding, bioturbation	Semi-closed lagoon	
M, W, P, G	Peloids, oncoids, ooids, bioclasts	Echinoderms, brachiopods, bivalves, gastropods, red algae, corals, benthic forams	Bioturbation	Open lagoon	Open lagoon
P, G, F, R	Ooids, oncoids, peloids, bioclasts, lithoclasts, soft pebbles	Benthic forams, gastropods	Cross-bedding, flaser bedding	Ooid shoal (active or abandoned)	Ooid shoal
B	Bioclasts	Corals, sponges, red algae, bryozoans, microencrusters	Bioperforation	Coral reef	Coral reef
	Up to 20% quartz, clays	Plant fragments		Terrigenous material	Terrigenous input
	Dolomite or dedolomite crystals, gypsum/anhydrite pseudomorphs	Plant fragments	Microbial lamination	Penecontemporaneous dolomitization overprinting tidal-flat or lagoonal facies	Dolomitization

the small-scale and elementary sequences (Strasser *et al.*, 1999).

Although the facies patterns at first glance look random in space as well as in time, there are certain trends that can be noted (Fig. 7):

1) Restricted-lagoonal facies dominate in small-scale sequences 1 to 8 but are then replaced by more open-marine facies up to the transgressive deposits of sequence 16. This major change is related to the prominent transgressive surface at the base of the Hauptmumienbank and Steinebach members (Figs 2 and 5).

2) Ooid shoals occur throughout the platform but are

more often found in transgressive deposits than in high-stand deposits of small-scale sequences (18 versus 9 occurrences). Furthermore, as for more open-marine facies, they become more abundant after the major transgression at the base of the Hauptmumienbank and Steinebach members (sequence 9).

3) Coral reefs occur on and off (more often in the high-stand parts than in the transgressive ones) but always in the same palaeogeographic positions (in sections 9 and 6, and in the cluster of sections 2 and 3). Like the ooid shoals, coral reefs become more abundant after the important transgression at the base of sequence 9.

4) Tidal flats are found only in sections 6 and 7, and signs of subaerial exposure only in section 1.

5) Siliciclastic input occurs at irregular intervals all over the platform but is most pronounced in sequences 6, 7, and 8, and to a minor degree in sequences 12 and 13.

6) Significant penecontemporaneous dolomitization occurs only in sequences 4, 15, and 16, and is most pronounced in the highstand deposits of sequence 16 (below sequence boundary Ox 8; Fig. 5).

Due to the limited outcrop conditions, not all sections contain all sequences (Fig. 5). Therefore, no statistical analyses (e.g., Markov chain) of vertical and lateral facies transitions have been performed.

8 Discussion

8.1 Role of platform morphology

The strongly variable thicknesses of the depositional sequences in the studied sections (Fig. 5) can at least partly be explained by differential subsidence (Pittet, 1994), which locally accelerated creation of accommodation while in other locations less space was available for the accumulation of sediment or even uplift could occur. Especially the area around section 1 was a high, explaining the reduced thickness of this section and the absence of sequence 16. Another — at least temporary — high can be assumed in the region of sections 6 and 7 where tidal flats occur in sequences 4 and 5. On the other hand, depressions accommodated more sediment per time unit, and siliciclastics could be channeled through such troughs (Hug, 2003). As the encountered facies generally suggest shallow to very shallow depositional environments, it can be assumed that the thickness of a sequence is a rough proxy for accommodation space. From Figure 5 it thus appears that depocenters shifted through time and that occasionally there was a tilt of the substrate (for example sequence 12, which is thin in section 6 and thickens significantly towards section 10).

Synsedimentary tectonics during the Oxfordian have also been invoked by Allenbach (2001) who found that the

differentiation into platforms and shallow basins switched with time. During the late Middle Oxfordian, subsidence accelerated in the southwestern part of the study area and depocenters developed in vicinity of faults within the basement. However, no faults cutting through the Jurassic sedimentary cover have been observed so far. It is assumed that the Triassic evaporites below deformed plastically; in this way, vertical movements within the basement resulted in flexures of the overlying sediments. Locally opposing palaeocurrent directions encountered in the Effingen Member (Fig. 2) indicate that the subsidence of the whole area was not continuous but that individual blocks had their own subsidence history (e.g., Bolliger and Burri, 1970; Wetzel and Allia, 2000). This is consistent with the position of the Jura Platform on the northern passive margin of the Tethys Ocean (Wildi *et al.*, 1989).

Besides the structuring of the platform by block faulting, also the irregular distribution of sediment bodies created morphology. Coral reefs and ooid shoals that possibly initiated on a structural high could migrate over the platform and — especially if early fresh-water diagenesis during a sea-level lowstand allowed for rapid cementation — create new, this time sedimentary highs. Structural and sedimentary highs redirected the oceanic and tidal currents and could isolate lagoons behind reef barriers or ooid shoals. This in turn could affect the water quality and, consequently, the ecological conditions for the carbonate-producing organisms.

In Figure 8, hypothetical cross-sections demonstrate how the platform originally was structured by block-faulting and how — throughout a sea-level cycle — facies may have shifted laterally. The vertical superpositions of facies reflect some of the situations that can be found in the studied sections (Fig. 5). However, it has to be considered that the platform was not only structured through (more or less) E-W trending synsedimentary faults but also through N-S striking ones. This created a complex pattern of compartments that moved more or less independently, producing depressions and highs in different palaeogeographic positions across the platform and thus explaining the often contrasted juxtapositions of facies seen in Figure 7.

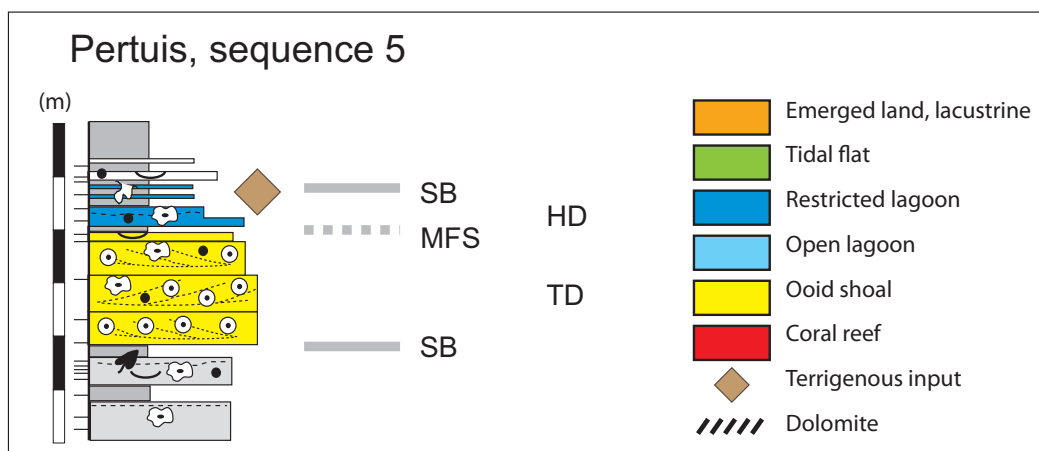


Figure 6 Left: Example of attribution of facies categories dominating the transgressive and the regressive parts of a small-scale sequence. SB: sequence boundary; MFS: maximum-flooding surface; TD: transgressive deposits; HD: highstand deposits. Right: legend to facies maps of Figure 7.

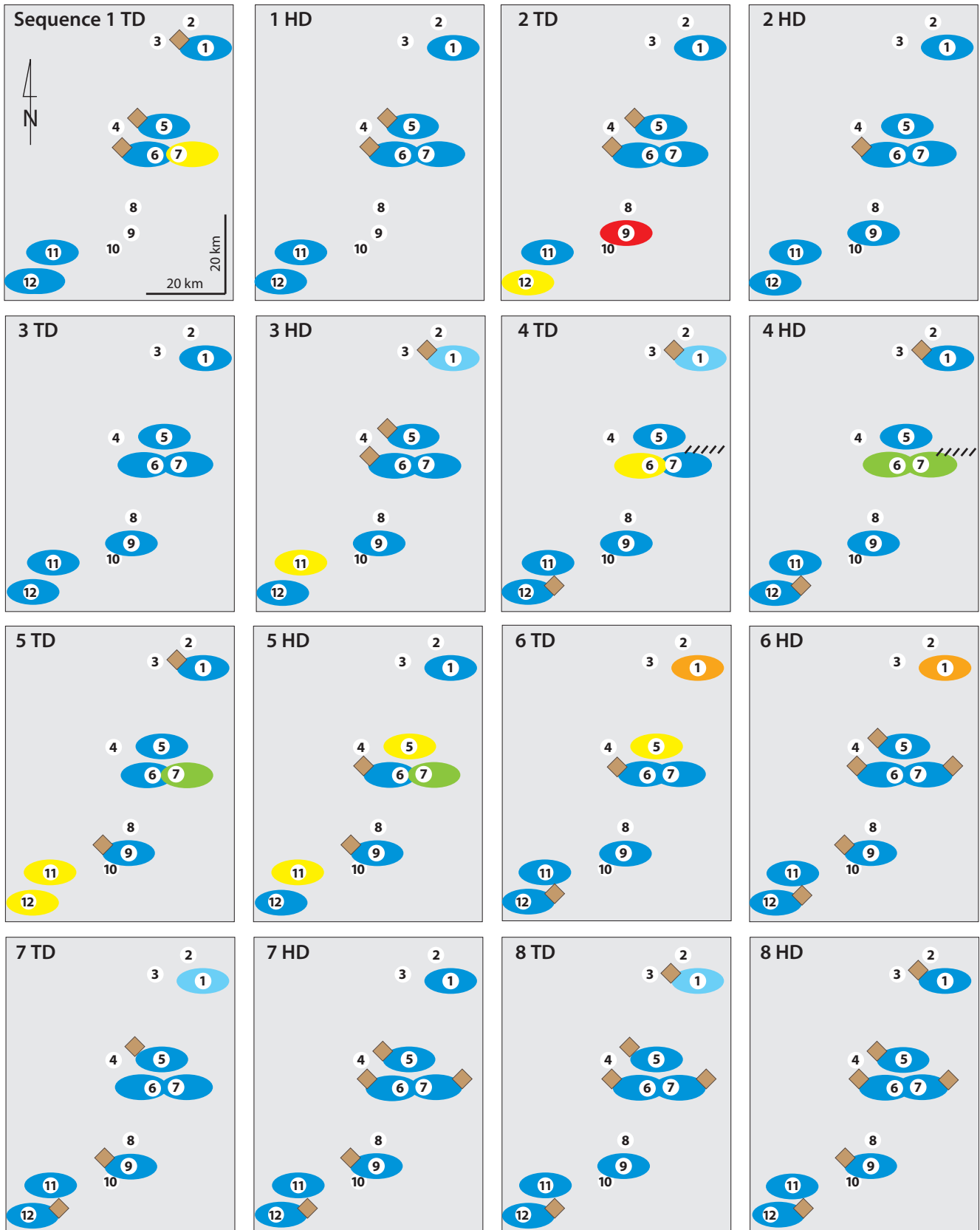


Figure 7 Palinspastic maps of sections 1 to 12, showing the dynamic facies evolution of the Jura Platform. Small-scale sequences 1 to 16 (defined in Fig. 5) have been subdivided into transgressive (TD) and highstand deposits (HD), and the dominant facies categories have been plotted (legend in Fig. 6).

8.2 Role of sea-level changes, climate, and currents

Besides subsidence, the second important factor controlling accommodation and thus sediment accumulation is eustatic sea level. The hierarchical stacking of different orders of depositional sequences observed in the studied sections and the chronostratigraphic frame suggest that the high-frequency sea-level changes were controlled by insolation changes in the Milankovitch frequency band (see chapter 5). As estimated from decompacted small-scale sequences, the amplitudes of sea-level fluctuations in tune with the 100-ka short eccentricity cycle were in the order of a few meters (Pittet, 1994; Strasser *et al.*, 2004, 2012). In the Late Jurassic, ice in high latitudes and altitudes probably was present (Eyles, 1993; Fairbridge, 1976; Frakes *et al.*, 1992) but ice volumes were small and glacio-eustatic fluctuations of low amplitude. However, orbitally-induced climate changes also caused thermal expansion and retraction of the uppermost layer of ocean water (*e.g.*, Gornitz *et al.*, 1982; Wigley and Raper, 1987), thermally-induced volume changes in deep-water circulation (Schulz and Schäfer-Neth, 1998), and/or water retention and release in lakes and aquifers (Jacobs and Sahagian, 1993). These processes contributed to high-frequency, low-amplitude sea-level changes (Conrad, 2013; Plint *et al.*, 1992).

Ooid shoals are found preferentially in the transgressive parts of the small-scale sequences (18 out of 27 occurrences; Fig. 7), probably because tidal currents were most active when water depth was shallow after the initial flooding of the previously very shallow or subaerially exposed substrate. On the other hand, coral reefs occur more often in the highstand deposits of the small-scale sequences (5 out of 7 occurrences; Fig. 7). Apparently they needed a minimum water depth that in many places was only attained after maximum flooding, and they preferred a grainy substrate over a muddy one. It is interesting to compare sequence 9 in sections 9 and 6 (Fig. 5): in section 9, the coral reef sits on lagoonal, oncoidal packstone and is covered with oolite, while in section 6 the reef grew on an ooid shoal. In the first case, the oncoid lagoon offered enough hard grains and/or incipient hardgrounds to allow settlement of the coral planula (*e.g.*, Hillgärtner *et al.*, 2001). In the second case it has to be assumed that the mobile shoal was stabilized (for example by dropping below the action of the tidal currents and subsequent incipient hardground formation) before the planula could successfully settle. Low sedimentation rates that allowed for hardground formation were possibly related to high-frequency sea-level changes that created the elementary sequences, and/or to lateral migration of depocenters.

Climate changes influenced rainfall over the exposed Hercynian massifs in the hinterland and thus terrigenous input of siliciclastics and nutrients. Clays and detrital quartz first accumulated in the deltas along the coasts (Fig. 1) and then were ponded in depressions and reworked by currents before they arrived in the study area, explaining their irregular distribution (Figs 5 and 7). Dissolved nutrients travelled faster: in fact, Dupraz and Strasser (1999, 2002) showed that the Oxfordian coral reefs in the Swiss Jura were first covered by microbialites resulting from nu-

trient excess before they were smothered by siliciclastics.

In the Late Oxfordian, evaporite pseudomorphs are locally found to be contemporaneous with increased siliciclastic input. This implies that either the siliciclastics were furnished during a humid phase and then redistributed during more arid conditions, or else that rainfall occurred above the crystalline massifs to the north whereas the carbonate platform further to the south was situated in a more arid climate belt (Hug, 2003). A palaeolatitudinal control on the distribution of siliciclastics was demonstrated by Pittet (1996) and Pittet and Strasser (1998) with high-resolution correlations between the Swiss Jura and Spain: while siliciclastics in the Jura concentrate rather around the boundaries of small- and medium-scale sequences, they occur in the transgressive or maximum-flooding intervals in the time-equivalent sequences of the Spanish sections.

8.3 A matter of scale

When comparing the time resolution of 50 ka to monitor the evolution of a carbonate platform as in this example from the Swiss Jura with the rate of environmental changes seen today on recent carbonate platforms, it becomes clear that only a very crude picture of the past can be drawn. The same holds for the resolution in space because outcrop conditions in the Swiss Jura do not allow for logging many closely-spaced and long sections that can be interpreted in terms of sequence- and cyclostratigraphy, nor for following lateral facies changes over more than a few tens of meters. The comparison of the palinspastic map of the Jura with satellite images of Belize and the Bahamas makes this discrepancy well visible (Fig. 9). While the ooid shoals of Joulter Cays occupy an area that is comparable to that covered by several sections in the Swiss Jura, the details of tidal channels and small islands are lost. In Belize, the complex pattern of elongated islands and lagoons cannot be reproduced by the sections that describe the Jura Platform. However, the facies distribution shown in Figure 7 implies that similar facies mosaics must have existed in the Oxfordian as are described from the modern platforms such as found in the Bahamas (*e.g.*, Rankey and Reeder, 2010) or in Belize (*e.g.*, Purdy and Gischler, 2003).

9 Conclusions

Conventional palaeogeographic maps of carbonate platforms are important to indicate their position with respect to land masses and ocean basins, to place them at a certain palaeolatitude, and to draft a rough distribution of sedimentary facies. However, such maps often are time-averaged over millions of years and therefore cannot monitor the complex facies evolution through space and through time. In the Oxfordian sedimentary record of the Swiss Jura Mountains, a high-resolution sequence- and cyclostratigraphic framework is available, which allows following a 1.6 Ma history of a shallow, subtropical, carbonate-dominated platform with time-steps of about 50 ka. Based on the facies analysis of 12 sections logged at cm-scale and on the palinspastic positioning of these sections on the platform, the following conclusions can be drawn:

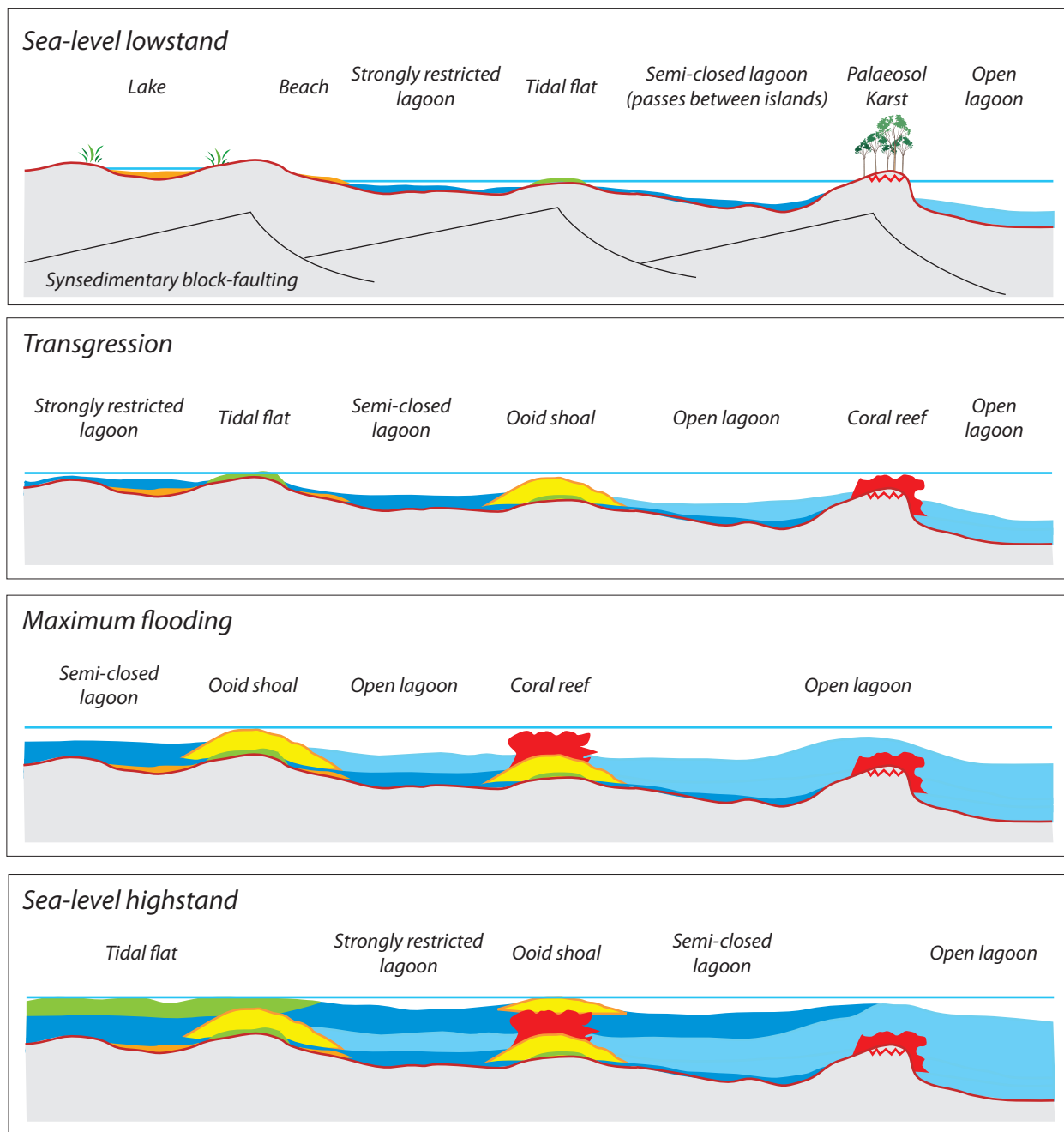


Figure 8 Sketches of facies distribution on a hypothetical carbonate platform structured by synsedimentary faulting. Situations during sea-level lowstand, transgression, maximum flooding, and sea-level highstand are inspired from the superposition and juxtaposition of facies as shown in Figures 5 and 7.

- Platform morphology created through synsedimentary block-faulting determined the position of islands, tidal flats, ooid shoals, and coral reefs that installed themselves preferentially on highs.
- Through migration of reefs and shoals and their rapid stabilization, also sedimentary highs were created.
- The highs were separated by depressions, in which clays accumulated to form marly deposits, and where the ecological conditions for the carbonate-producing organisms were partly or fully restricted (in terms of water energy and/or oxygenation).
- High-frequency sea-level changes in tune with the or-

- bital cycles of short (100 ka) and long (400 ka) eccentricity controlled at least partly the vertical facies evolution of depositional sequences (deepening-shallowing trends).
- While facies distribution through space and time at first glance looks random, some trends can be seen: ooid shoals preferentially formed during transgression, while coral reefs are more common in highstand deposits.
- The effects of sea-level changes linked to the 20-ka precessional cycle are often difficult to demonstrate in the studied sections, as autocyclic processes were superimposed.
- Siliciclastic and nutrient input from the hinterland was controlled by sea-level and/or climatic changes and was

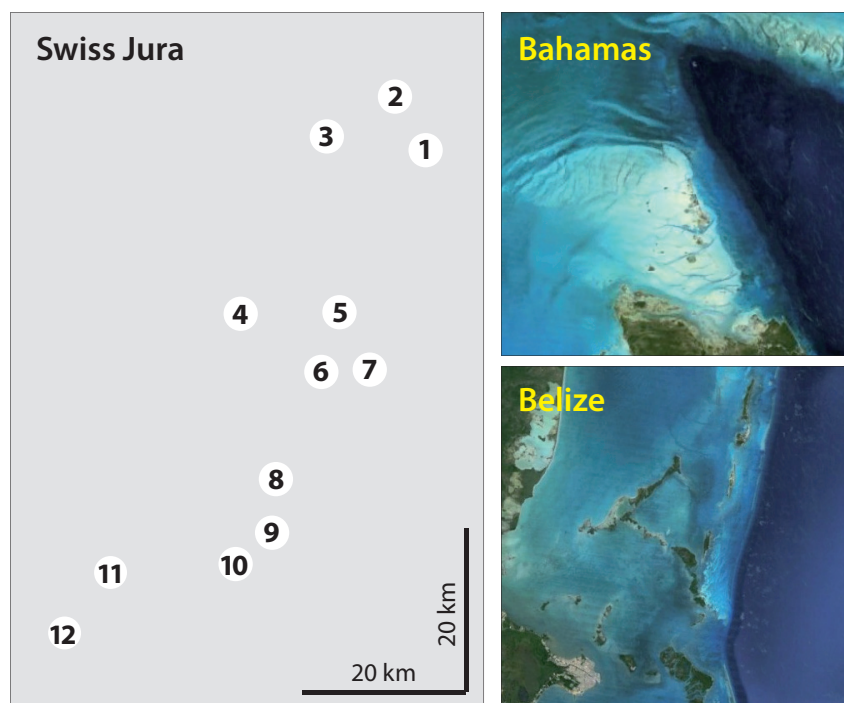


Figure 9 Comparison between the studied sections in the Swiss Jura (palinspastic map) and – at the same scale – examples of recent carbonate platforms in the Bahamas (white area: ooid shoals of Joultier Cays) and Belize (Belize City on the promontory in lower left corner). Satellite images from Google Earth.

sporadically distributed by currents all over the platform.

– Co-occurrence of dolomite and siliciclastics suggests that climate may have been humid in the hinterland while it was arid on the studied platform.

– Coral reefs demised due to nutrient and siliciclastic input and were also influenced by sea-level changes. They recovered at regular intervals, albeit often in another location on the platform.

Although much detail may be gained through this type of analysis, it never can reflect the true history of a carbonate platform. This becomes evident when comparing the studied Jura Platform with the complex facies mosaics found on modern platforms such as the Bahamas or Belize. First, the spatial resolution of the outcrops is not dense enough to monitor lateral facies changes at the scale of tens or hundreds of meters as they commonly occur today and also occurred in the past (as shown punctually in some outcrops in the Swiss Jura). Second, the time resolution of 50 ka is hypothetical and depends on the validity of the correlations between the sections. Furthermore, facies changes through time happen (and happened) on time-scales of days (if induced by storms) to tens, hundreds, or a few thousands of years, which is much faster than the hypothetical 50 ka. Consequently, shorelines, reefs, and shoals could have shifted, islands could have appeared and disappeared, without leaving a trace in the visible sedimentary record.

The present study shows the potential that a detailed facies analysis, supported by sequence- and cyclostratigraphy, can offer towards a better representation of palaeogeography. On the other hand, we are still far from being able to reconstruct all the features of the Jura Platform, which certainly was as complex as any modern carbonate

system.

Acknowledgements

This study is based on research carried out with the financial support of the Swiss National Science Foundation, which is gratefully acknowledged (Projects No. 20–41888, 20–43150, 20–46625, 20–67736, and 20–109214). We thank Ian D. Somerville who invited us to present our results at the IAS International Sedimentological Congress in Geneva. We also thank Tom van Loon and an anonymous reviewer for their constructive comments on the first version of the manuscript.

References

1. Allenbach, R., 2001. Synsedimentary tectonics in an epicontinental sea: a new interpretation of the Oxfordian basins of northern Switzerland. *Eclogae Geologicae Helveticae*, 94, 265–287.
2. Barron, E.J., Harrison, C.G.A., Sloan, J.L. II, Hay, W.W., 1981. Paleogeography, 180 million years to present. *Eclogae Geologicae Helveticae*, 74, 443–470.
3. Bitterli, T., 1990. The kinematic evolution of a classical Jura fold: a reinterpretation based on 3–dimensional balancing techniques (Weissenstein Anticline, Jura Mountains, Switzerland). *Eclogae Geologicae Helveticae*, 83, 493–511.
4. Blakey, R.C., 2014. Paleogeographic maps. Cpgeosystems.com/paleomaps.html.
5. Bolliger, W., Burri, P., 1970. Sedimentologie von Shelf-Carbonaten und Beckenablagerungen im Oxfordien des zentralen Schweizer Jura. *Beiträge Geologische Karte Schweiz*, N.F. 140.

6. Carpentier, C., Martin-Garin, B., Lathuilière, B., Ferry, S., 2006. Correlation of reefal Oxfordian episodes and climatic implications in the eastern Paris Basin (France). *Terra Nova*, 18, 191–201.
7. Clari, P.A., Dela Pierre, F., Martire, L., 1995. Discontinuities in carbonate successions: identification, interpretation and classification of some Italian examples. *Sedimentary Geology*, 100, 97–121.
8. Conrad, C.P., 2013. The solid Earth's influence on sea level. *GSA Bulletin*, 125, 1027–1052.
9. Dercourt, J., Ricou, L.E., Vrielynck, B. (Eds.), 1993. Tethys Palaeoenvironmental Maps. Gauthier-Villars, Paris.
10. Dupraz, C., 1999. Paléontologie, paléocologie et évolution des faciès récifaux de l'Oxfordien moyen-supérieur (Jura suisse et français). *GeoFocus*, 2, 1–247.
11. Dupraz, C., Strasser, A., 1999. Microbialites and micro-encrusters in shallow coral bioherms (Middle to Late Oxfordian, Swiss Jura Mountains). *Facies*, 40, 101–130.
12. Dupraz, C., Strasser, A., 2002. Nutritional modes in coral-microbialite reefs (Jurassic, Oxfordian, Switzerland): evolution of trophic structure as a response to environmental change. *Palaios*, 17, 449–471.
13. Dunham, R.G., 1962. Classification of carbonate rocks according to depositional texture. *AAPG Memoir*, 1, 108–121.
14. Enay, R., Contini, D., Boullier, A., 1988. Le Séquanien-type de Franche-Comté (Oxfordien supérieur): datations et corrélations nouvelles, conséquences sur la paléogéographie et l'évolution du Jura des régions voisines. *Eclogae Geologicae Helvetiae*, 81, 295–363.
15. Eyles, N., 1993. Earth's glacial record and its tectonic setting. *Earth-Science Reviews*, 35, 1–248.
16. Fairbridge, R.W., 1976. Convergence of evidence on climatic change and ice ages. *Annals of the New York Academy of Science*, 91, 542–579.
17. Frakes, L.A., Francis, J.E., Syktus, J.I., 1992. Climate Modes of the Phanerozoic. Cambridge University Press, 1–274.
18. Gornitz, V., Lebedeff, S., Hansen, J., 1982. Global sea-level trend in the past century. *Science*, 215, 1611–1614.
19. Gradstein, F.M., Agterberg, F.P., Ogg, J.G., Hardenbol, J., van Veen, P., Thierry, J., Huang, Z., 1995. A Triassic, Jurassic and Cretaceous time scale. *SEPM Special Publication*, 54, 95–126.
20. Gsponer, P., 1999. Etude géologique et sédimentologique de l'anticlinal du Chasseral dans la région de La Heutte. Unpublished diploma thesis, University of Fribourg, 1–107.
21. Gygi, R.A., 1969. Zur Stratigraphie der Oxford-Stufe (oberes Jura-System) der Nordschweiz und des süddeutschen Grenzgebietes. Beiträge Geologische Karte Schweiz, N.F. 136.
22. Gygi, R.A., 1992. Structure, pattern of distribution and paleobathymetry of Late Jurassic microbialites (stromatolites and oncoids) in northern Switzerland. *Eclogae Geologicae Helvetiae*, 85, 799–824.
23. Gygi, R.A., 1995. Datierung von Seichtwassersedimenten des Späten Jura in der Nordwestschweiz mit Ammoniten. *Eclogae Geologicae Helvetiae*, 88, 1–58.
24. Gygi, R.A., 2000. Integrated stratigraphy of the Oxfordian and Kimmeridgian (Late Jurassic) in northern Switzerland and adjacent southern Germany. *Memoir of the Swiss Academy of Sciences*, 104, 1–152.
25. Gygi, R.A., Coe, A.L., Vail, P.R., 1998. Sequence stratigraphy of the Oxfordian and Kimmeridgian stages (Late Jurassic) in northern Switzerland. *SEPM Special Publication*, 60, 527–544.
26. Gygi, R.A., Persoz, F., 1986. Mineralostratigraphy, litho- and biostratigraphy combined in correlation of the Oxfordian (Late Jurassic) formations of the Swiss Jura range. *Eclogae Geologicae Helvetiae*, 79, 385–454.
27. Hardenbol, J., Thierry, J., Farley, M.B., Jacquin, T., De Graciansky, P.-C., Vail, P.R., 1998. Charts. *SEPM Special Publication*, 60.
28. Hill, J., Wood, R., Curtis, A., Tetzlaff, D.M., 2012. Preservation of forcing signals in shallow water carbonate sediments. *Sedimentary Geology*, 275–276, 79–92.
29. Hillgärtner, H., 1998. Discontinuity surfaces on a shallow-marine carbonate platform (Berriasian – Valanginian, France and Switzerland). *Journal of Sedimentary Research*, 68, 1093–1108.
30. Hillgärtner, H., Dupraz, C., Hug, W., 2001. Microbially induced cementation of carbonate sands: are micritic meniscus cements good indicators of vadose diagenesis? *Sedimentology*, 48, 117–131.
31. Hindle, D., Burkhard, M., 1999. Strain, displacement and rotation associated with the formation of curvature in fold belts; the example of the Jura arc. *Journal of Structural Geology*, 21, 1089–1101.
32. Hug, W. A., 2003. Sequenzielle Faziesentwicklung der Karbonatplattform des Schweizer Jura im Späten Oxford und frühesten Kimmeridge. *GeoFocus*, 7, 1–156.
33. International Commission on Stratigraphy, 2014. International chronostratigraphic chart. <http://www.stratigraphy.org/index.php/ics-chart-timescale>.
34. Jacobs, D.K., Sahagian, D.L., 1993. Climate-induced fluctuations in sea level during non-glacial times. *Nature*, 361, 710–712.
35. Jank, M., Meyer, C.A., Wetzel, A., 2006. Late Oxfordian to Late Kimmeridgian carbonate deposits of NW Switzerland (Swiss Jura): stratigraphical and palaeogeographical implications in the transition area between the Paris Basin and the Tethys. *Sedimentary Geology*, 186, 237–263.
36. Jordan, P., 1999. Géologie de la région de Montoz (Jura bernois) avec analyse séquentielle de deux profils de l'Oxfordien moyen et supérieur. Unpublished diploma thesis, University of Fribourg, 1–104.
37. Montañez, I.A., Osleger, D.A., 1993. Parasequence stacking patterns, third-order accommodation events, and sequence stratigraphy of Middle to Upper Cambrian platform carbonates, Bonanza King Formation, southern Great Basin. *AAPG Memoir*, 57, 305–326.
38. Mosar, J., 1999. Present-day and future tectonic underplating in the western Swiss Alps: reconciliation of basement/wrench-faulting and décollement folding of the Jura and Molasse basin in the Alpine foreland. *Earth and Planetary Science Letters*, 173, 143–155.
39. Pittet, B., 1994. Modèle d'estimation de la subsidence et des variations du niveau marin: un exemple de l'Oxfordien du Jura suisse. *Eclogae geologicae Helvetiae*, 87, 513–543.
40. Pittet, B., 1996. Contrôles climatiques, eustatiques et tectoniques sur des systèmes mixtes carbonates-siliciclastiques de plate-forme: exemples de l'Oxfordien (Jura suisse, Normandie, Espagne). PhD thesis, University of Fribourg, 1–258.
41. Pittet, B., Strasser, A., 1998. Long-distance correlations by sequence stratigraphy and cyclostratigraphy: examples and implications (Oxfordian from the Swiss Jura, Spain, and Normandy). *Geologische Rundschau*, 86, 852–874.
42. Plint, A.G., Eyles, N., Eyles, C.H., Walker, R.G., 1992. Control of sea level change, in: Walker, R.G., James, N.P. (Eds.), *Facies Models – Response to Sea Level Change*. Geological Association of Canada, pp. 15–25.
43. Purdy, E.G., Gischler, E., 2003. The Belize margin revisited: 1. Holocene marine facies. *International Journal of Earth Sciences*, 92, 532–551.
44. Rankey, E.C., Reeder, S.L., 2010. Controls on platform-scale patterns of surface sediments, shallow Holocene platforms, Bahamas. *Sedimentology*, 57, 1545–1565.
45. Rauber, G., 2001. Géologie de la région de Bärschwil-Grindel (Jura soleurois, Suisse) avec analyse détaillée dans l'Oxfordien

- supérieur. Unpublished diploma thesis, University of Fribourg, 1–94.
46. Samankassou, E., Strasser, A., Di Gioia, E., Rauber, G., Dupraz, C., 2003. High-resolution record of lateral facies variations on a shallow carbonate platform (Upper Oxfordian, Swiss Jura Mountains). *Eclogae Geologicae Helveticae*, 96, 425–440.
 47. Schulz, M., Schäfer-Neth, C., 1998. Translating Milankovitch climate forcing into eustatic fluctuations via thermal deep water expansion: a conceptual link. *Terra Nova*, 9, 228–231.
 48. Scotese, C.R., 2014. Paleomap project. www.scotese.com.
 49. Smith, G.A., Smith, D.G., Funnell, B.M. 1994. Atlas of Mesozoic and Cenozoic Coastlines. Cambridge University Press.
 50. Stampfli, G.M., Borel, G.D., 2002. A plate tectonic model for the Paleozoic and Mesozoic constrained by dynamic plate boundaries and restored synthetic oceanic isochrons. *Earth and Planetary Science Letters*, 196, 17–33.
 51. Stampfli, G.M., Hochard, C., Verard, C., Wilhem, C., von Raumer, J., 2013. The formation of Pangea. *Tectonophysics*, 593, 1–19.
 52. Stienne, N., 2010. Paléocéologie et taphonomie comparative en milieux carbonates peu profonds (Oxfordien du Jura Suisse et Holocène du Belize). *GeoFocus*, 22, 1–248.
 53. Strasser, A., 1991. Lagoonal-peritidal sequences in carbonate environments: autocyclic and allocyclic processes, in: Einsele, G., Ricken, W., Seilacher, A. (Eds.), *Cycles and Events in Stratigraphy*, pp. 709–721.
 54. Strasser, A., 2007. Astronomical time scale for the Middle Oxfordian to Late Kimmeridgian in the Swiss and French Jura Mountains. *Swiss Journal of Geosciences*, 100, 407–429.
 55. Strasser, A., Hillgärtner, H., 1998. High-frequency sea-level fluctuations recorded on a shallow carbonate platform (Berriasian and Lower Valanginian of Mount Salève, French Jura). *Eclogae Geologicae Helveticae*, 91, 375–390.
 56. Strasser, A., Hillgärtner, H., Pasquier, J.-B., 2004. Cyclostratigraphic timing of sedimentary processes: an example from the Berriasian of the Swiss and French Jura Mountains. *SEPM Special Publication*, 81, 135–151.
 57. Strasser, A., Pittet, B., Hillgärtner, H., Pasquier, J.-B., 1999. Depositional sequences in shallow carbonate-dominated sedimentary systems: concepts for a high-resolution analysis. *Sedimentary Geology*, 128, 201–221.
 58. Strasser, A., Védryne, S., 2009. Controls on facies mosaics of carbonate platforms: a case study from the Oxfordian of the Swiss Jura. *IAS Special Publication*, 41, 199–213.
 59. Strasser, A., Védryne, S., Stienne, N., 2012. Rate and synchronicity of environmental changes on a shallow carbonate platform (Late Oxfordian, Swiss Jura Mountains). *Sedimentology*, 59, 185–211.
 60. Thierry, J., 2000. Early Kimmeridgian (146–144 Ma), in: Der-court, J., Gaetani, M., Vrielynck, B., Barrier, E., Biju-Duval, B., Brunet, M.F., Cadet, J.P., Crasquin, S., Sandulescu, M. (Eds.), *Atlas Peri-Tethys*, Map 10. CCGM/CGMW, Paris.
 61. Ustaszewski, K., Schmid, S.M., 2006. Control of preexisting faults on geometry and kinematics in the northernmost part of the Jura fold-and-thrust belt. *Tectonics*, 25, TC5003.
 62. Vail, P.R., Audemard, F., Bowen, S.A., Eisner, P.N., Perez-Cruz, C., 1991. The stratigraphic signatures of tectonics, eustasy and sedimentology – an overview, in: Einsele, G., Ricken, W., Seilacher, A. (Eds.), *Cycles and Events in Stratigraphy* pp. 617–659.
 63. Védryne, S., 2007. High-frequency palaeoenvironmental changes in mixed carbonate-siliciclastic sedimentary systems (Late Oxfordian, Switzerland, France, and southern Germany). *GeoFocus*, 19, 1–216.
 64. Védryne, S., Strasser, A., 2009. High-frequency palaeoenvironmental changes on a shallow carbonate platform during a marine transgression (Late Oxfordian, Swiss Jura Mountains). *Swiss Journal of Geosciences*, 102, 247–270.
 65. Wetzel, A., Allia, V., 2000. The significance of hiatus beds in shallow-water mudstones: an example from the Middle Jurassic of Switzerland. *Journal of Sedimentary Research*, 70, 170–180.
 66. Wetzel, A., Allia, V., Gonzalez, R., Jordan, P., 1993. Sedimentation und Tektonik im Ostjura. *Eclogae Geologicae Helveticae*, 86, 313–332.
 67. Wigley, T.M.L., Raper, S.C.B., 1987. Thermal expansion of sea water associated with global warming. *Nature*, 330, 127–131.
 68. Wildi, W., Funk, H., Loup, B., Amato, E., Huggenberger, P., 1989. Mesozoic subsidence history of the European marginal shelves of the Alpine Tethys (Helvetic realm, Swiss Plateau and Jura). *Eclogae Geologicae Helveticae*, 82, 817–840.
 69. Wilkinson, B.H., Drummond, C.N., 2004. Facies mosaics across the Persian Gulf and around Antigua – stochastic and deterministic products of shallow-water sediment accumulation. *Journal of Sedimentary Research*, 74, 513–526.
 70. Ziegler, M.A., 1962. Beiträge zur Kenntnis des unteren Malm im zentralen Schweizer Jura. PhD thesis, University of Zurich.
 71. Ziegler, P.A., 1956. Geologische Beschreibung des Blattes Courtelary (Berner Jura), und zur Stratigraphie des Sequanien im zentralen Schweizer Jura. Beiträge geologische Karte Schweiz, N.F. 102.
 72. Ziegler, P.A., 1988. Evolution of the Arctic – North Atlantic and the Western Tethys. *AAPG Memoir*, 43 (charts).

(Edited by Yuan Wang)